New Journal of Physics
The open-access journal for physics

Exciton–polaritons in a ZnO-based microcavity: polarization dependence and nonlinear occupation

Chris Sturm[1], **Helena Hilmer, Rüdiger Schmidt-Grund and Marius Grundmann**

Universität Leipzig, Institut für Experimentelle Physik II, Linnéstrasse 5, 04103 Leipzig, Germany
E-mail: csturm@physik.uni-leipzig.de

New Journal of Physics **13** (2011) 033014 (17pp)
Received 15 October 2010
Published 8 March 2011
Online at http://www.njp.org/
doi:10.1088/1367-2630/13/3/033014

Abstract. We report on the occupation of the lower exciton–polariton branch in a ZnO-based microcavity as a function of the detuning between the exciton and the uncoupled cavity-photon mode and on the optical excitation density. We emphasize the difference in the dispersion and occupation of the lower polariton branch as a function of the linear polarization of the emitted light. For the negative detuning regime, we found an energy splitting between the transverse electric (TE)- and transverse magnetic (TM)-polarized states at in-plane wave vectors between $0.4 \times 10^7\,\mathrm{m}^{-1}$ and $1.2 \times 10^7\,\mathrm{m}^{-1}$, which is caused by the polarization dependence of the dispersion of the uncoupled cavity-photon mode. The maximum energy splitting of about 6 meV was observed for a detuning of about $\Delta = -70$ meV. From the integrated photoluminescence peak, we deduce the occupation of the lower polariton branch as well as the scattering rates of exciton–polaritons into the lower polariton branch. We found that the energy splitting causes an enhanced scattering of exciton–polaritons into the lower polariton branch for the TM-polarized light compared with that of the TE-polarized light. By varying the excitation density, we observe a superlinear growth of the lower polariton branch occupation for negative and intermediate detuning regimes. For an accumulation of exciton–polaritons in the ground state at low temperatures ($T = 10$ K), we found an intermediate detuning regime (-20 meV $< \Delta < +20$ meV) as the optimum. With increasing temperature, this optimum detuning range shifts to larger negative values.

[1] Author to whom any correspondence should be addressed.

Contents

1. Introduction

In recent years, planar microcavities have been in the scope of interest, since they allow us to investigate and manipulate light–matter coupling (see e.g. [1, 2]). In the strong light–matter coupling regime, the coupling forms bosonic quasi-particles, the so-called exciton–polaritons. These particles allow the realization of new devices based on exciton–polariton emission, such as optical amplifiers [3, 4], polariton LEDs [5] and ultra-low-threshold lasers [6]. Furthermore, these particles can undergo Bose–Einstein condensation (BEC) at elevated temperatures [7, 8].

In addition to the well-established material systems for microcavities, such as GaAs and CdTe [1, 7, 9], materials with a large exciton binding energy are of special interest since they allow the realization of the strong coupling regime at elevated temperatures. Therefore, ZnO is a promising candidate since it has the highest predicted critical temperature [10] and the strong coupling regime was observed up to 410 K [11]. Furthermore, the critical temperature at which a BEC can occur in such microcavities was predicted to be $T = 610$ K [10]. This is the highest proposed critical temperature for microcavities. However, the observation of a BEC in ZnO-based microcavities has not been reported so far. Essential for the realization of a BEC is a massive occupation of the ground state with exciton–polaritons, caused by the relaxation or rather scattering of excited exciton–polaritons. This process depends, on the one hand, on the properties of the active medium, such as the phonon energies and the exciton binding energy and, on the other hand, it can be influenced by the temperature, the excitation density and the detuning, i.e. the difference in the uncoupled cavity-photon and exciton energy. The last one is a measure of the steepness of the exciton–polariton dispersion. For the optimal detuning regime for the realization of a BEC in ZnO-based microcavities, there are two opposite statements. Butté *et al* [12] found for GaN-based microcavities, which should be similar to ZnO-based ones, that a large negative detuning is preferred for the realization of BEC. In contrast to that, calculations by Johne *et al* [33] for ZnO-based microcavities yield a positive detuning regime as optimal for the realization of a BEC at room temperature. In order to find an answer to this contradiction, we investigated the occupation of the exciton–polaritons in a planar ZnO-based microcavity as a function of the detuning, the polarization and the excitation density.

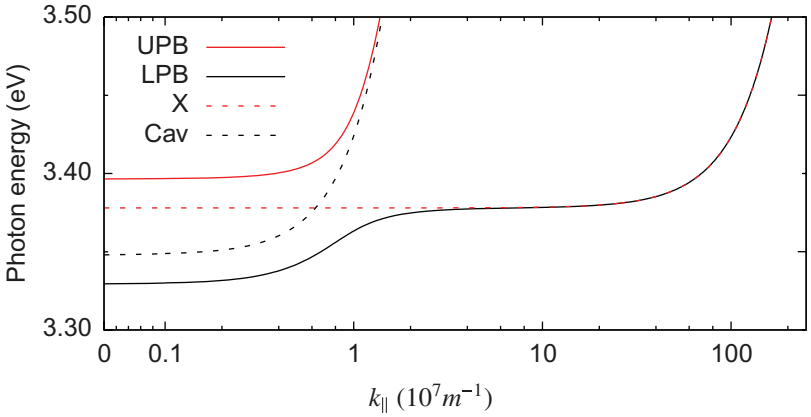

Figure 1. Dispersion behaviour of the exciton–polariton branches (solid lines) for a negative detuning ($\Delta = -2V = -60\,\text{meV}$). The dotted lines represent the dispersion of the exciton and cavity-photon mode in the uncoupled regime. The effective mass, which was used for the calculation of the exciton mode dispersion, was set to that of the ZnO exciton [13]. (We note, that the x-axis has a linear scale up to an in-plane wave vector of $10^6\,\text{m}^{-1}$).

2. Exciton–polaritons in planar microcavities

The cavity layer in a planar microcavity, which is embedded between two Bragg reflectors (BR), leads to a perturbation of the photonic band structure and the formation of a defect mode in the one-dimensional photonic band gap. This defect mode is usually called the cavity-photon mode. In contrast to the linear dispersion of the photon in vacuum or a homogeneous medium, the dispersion of the cavity-photon mode has parabolic behaviour. The strong coupling of this mode with an exciton leads to the formation of exciton–polaritons: in the simplest case, the coupling between one cavity-photon and one exciton. For this situation, the dispersion of the exciton–polaritons consists of two branches: a lower polariton branch (LPB) and an upper polariton branch (UPB). The characteristic of each branch and the corresponding exciton–polaritons are determined by the energy difference between the uncoupled modes, i.e. $\delta(k_{\|}) = E_{\text{Cav}}(k_{\|}) - E_{\text{X}}(k_{\|})$. For a negative δ, the LPB has a photonic characteristic and therefore the properties of the exciton–polaritons, such as the lifetimes, that correspond to this branch are mainly determined by the uncoupled cavity-photon. The UPB and therefore the corresponding exciton–polaritons have complementary characteristic compared with the LPB. For a positive δ, the situation changes and the LPB has excitonic characteristic whereas the UPB has a photonic one. At $\delta = 0\,\text{meV}$, the LPB as well as the UPB have the same characteristic, half-photonic and half-excitonic. At zero in-plane wave vector, the quantity δ is known as detuning Δ. The dispersion of both branches is schematically shown in figure 1 for a negative detuning of $\Delta = -2V$, with the coupling strength $V = 30\,\text{meV}$ and the energy of the exciton in ZnO.

For small in-plane wave vectors, the dependence of the exciton energy on the in-plane wave vector is negligible and is given by $E(k_{\|}) \approx E(k_{\|} = 0)$. In contrast to that, the energy of the uncoupled cavity photon depends strongly on its in-plane wave vector. Furthermore, the cavity-photon mode can be separated into two components that have an orthogonal linear polarization: namely the linear polarization parallel and perpendicular to the plane of incidence or rather to the plane of detection (see the inset of figure 3(b)). In this paper, the electrical field of the

transverse electric (TE)-polarized mode is parallel to the layer interfaces, i.e. perpendicular to the growth direction, whereas that of the transverse magnetic (TM)-polarized mode is a linear combination of the electric field parallel and perpendicular to the layer interfaces. At normal emission angle (or normal incidence), the component of the electrical field of the TM-polarized mode that is perpendicular to the layer interface vanishes and therefore the two polarized modes have degenerated. The photonic band structure and therefore the dispersion of the two polarized cavity-photon modes are different, and are determined by the properties of the BR [14, 15]. Therefore, an energy splitting between the two modes is observable for non-zero in-plane wave vectors. This splitting increases with increasing in-plane wave vector. In the picture of a photonic band structure, the branches of the cavity-photon mode can be treated as photonic bands with the corresponding polarization. In the following, these bands are labelled as TE and TM bands. If we consider the equivalent basis of circular polarization, the TE- and TM-polarized states can be transferred into left- and right-handed circular polarization. That means that both bands contain cavity photons with spin up and spin down, which can couple to the respective excitonic states. Besides the different energy dispersion of the TE and TM bands, the lifetime of the corresponding cavity photons is different. For the cavity polaritons of the TE band, the lifetime increases with increasing in-plane wave vector, whereas for cavity photons of the TM band, a decrease is observable. In the picture of a Fabry–Perot resonator, where the BRs act as mirrors, this can be understood by the fact that the reflectivity of the BR has a different dependence on the in-plane wave vector for the two polarizations.

In consequence, the exciton–polariton branches in the strong coupling regime, the LPB as well as the UPB, can also be separated into two orthogonal linear polarized components. For conventionally used microcavity materials, this splitting of the LPB is negligible and is typically less than 1 meV [14, 16]. In the case of ZnO-based microcavities, the two bands of the LPB are well resolved. Since the dispersion of the LPB as well as the lifetime of the respective exciton–polaritons differ for the two polarizations, differences in the relaxation process of the exciton–polaritons into the ground state are expected in ZnO-based microcavities. In the following, we will label the LPB that emits TE-polarized light as TE-LPB and that with the TM-polarized one accordingly TM-LPB (analogous to the labelling of the bands of the cavity-photon mode).

We note that, in addition to the discussed splitting of the cavity-photon mode, the longitudinal-transversal splitting of the excitons also has an influence on the spin dynamics of the exciton–polaritons [17]. Above a certain pump threshold, the exciton–polaritons at the ground state have a certain preferred spin polarization caused by the spin dynamics of the exciton–polariton scattering. In this paper, we will focus on the influence of linear polarization of the cavity-photon mode on exciton–polariton relaxation. Thereby, it cannot be distinguished between left- and right-handed circular polarization so that the spin dynamics of exciton–polariton scattering rates are omitted here.

3. Sample and experimental setup

We have investigated the relaxation process of exciton–polaritons in a ZnO-based microcavity deposited by pulsed laser deposition. The microcavity consists of a half medium wavelength intentionally wedge-shaped ZnO cavity (wurtzite structure), acting simultaneously as active medium (figure 2(a)). One advantage of the wedge-shaped cavity is that the detuning of the microcavity can be changed by variation of the spatial position on the microcavity. At $T = 10\,\mathrm{K}$,

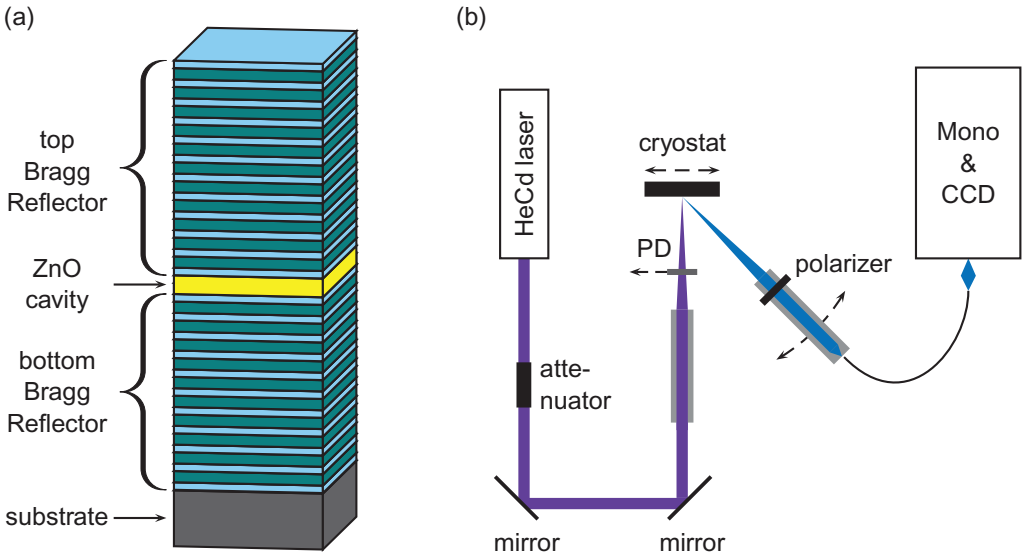

Figure 2. Schematic drawing of the sample structure (a) and of the experimental setup (b). The photodiode (PD) can be moved into the laser beam (violet) in order to control its intensity. The emitted light is depicted in blue.

a detuning regime between −70 meV and +60 meV can be adjusted. The cavity was embedded between two BRs, each made of 10.5 layer pairs of yttria-stabilized zirconia (YSZ) and alumina (Al_2O_3). For further information about the growth procedure (see [18]).

We deduce the scattering properties of the exciton–polaritons into an in-plane wave vector $k_\parallel$ from photoluminescence (PL) measurements for angles of emission (θ) in the range 0°–70°. Since it is common to relate the scattering properties to an in-plane wave vector instead of an angle, we convert the angle of emission into the in-plane wave vector by

$$k_\parallel = \frac{E(\theta)\sin\theta}{\hbar c}, \tag{1}$$

with the photon energy of the emitted light E, the vacuum velocity of light c and the reduced Planck constant $\hbar$. Therefore, the corresponding range of in-plane wave vectors is $(0\ldots1.2)\times10^7\,\mathrm{m}^{-1}$. We excite the microcavity with a HeCd laser (cw, 325 nm) at an angle of incidence of about 20° perpendicular to the plane of detection. In this configuration, we avoid the detection of laser light caused by reflection and provide a high-energy transfer into the cavity. The last one is ensured by the fact that the reflectivity of the top BR reaches a minimum value at the excitation wavelength for this angle. The emitted PL was collected by a lens (solid angle $\approx 9.6\times10^{-4}$ sr) and coupled into an optical fibre that guided the light to the spectrometer (focal length of 320 mm and a grating of 2400 l mm^{-1}) and a charge-coupled device (CCD) (figure 2(b)).

4. Results and discussion

4.1. Dispersion behaviour of the exciton–polariton branch

The PL spectra of the microcavity for a detuning of about $\Delta = -70$ meV at $T = 10$ K are shown in figure 3(a) for the TE-polarization. Two modes are observable: the first one at an energy

of about 3.29 eV and the second one at an energy of about 3.36 eV at normal emission. The dispersion behaviour of both modes is shown in figure 3(b), yielding complementary behaviour for the two modes. For small in-plane wave vectors, the energy of the first mode increases with increasing in-plane wave vector, whereas the energy of the second mode remains nearly constant. For large in-plane wave vectors, the opposite is the case. The observed behaviour of the first mode is typical for a microcavity that exhibits a strong coupling between the cavity photon and the free exciton (cf figure 1). However, the energy at which the first mode converges at high $k_{\parallel}$ values and that of the second mode at $k_{\parallel} = 0$ are close to that of the donor-bound excitons $E_{D_0X} \approx 3.36$ eV [19, 20]. This indicates that besides the strong coupling of the cavity-photon mode with the free exciton, also a coupling between the donor-bound exciton and the cavity-photon mode is present in this microcavity. In contrast to the free excitons, the donor-bound excitons are localized. Usually, they are responsible for the dominant peaks in the PL spectra of ZnO bulk single crystals and films at low temperatures [19, 20]. Due to their localization, they show electronic properties comparable with quantum dots. If the density of the donors exceeds a certain level, the wave functions of the bound electronic states start to overlap slightly and they behave similar to an ensemble of quantum dots with optical properties like a quantum well [21]. It is well known that the electronic states of such structures embedded in a microresonator can couple to the cavity-photon mode. A strong coupling of a single quantum dot with a cavity-photon mode was experimentally observed by Reithmaier *et al* and Yoshie *et al* [22, 23]. Usually the volume of donor-bound excitons is very small so that the coupling with a cavity-photon mode is negligible and much weaker than that with the free excitons. Furthermore, such low concentrations do not allow any propagation of the polaritons and the k-space distribution should be 1D like. This means that no intra-branch relaxation processes in the momentum and the energy space would be possible. For the microcavity presented here, the concentration of the donor-bound excitons seems to be large enough to yield a high enough coupling strength and wave function overlap, so that there is an intermediate coupling regime between the donor-bound excitons and the cavity-photon mode. Hereby the intermediate coupling regime denotes that the energy splitting between the first and the second mode at the crossing point ($k_{\parallel} \approx 1.15 \times 10^7\,\mathrm{m}^{-1}$) is less than the broadening of the corresponding modes. A detailed description of the coupling with the donor-bound excitons is not the aim of this paper and will be presented elsewhere. Nevertheless, we interpret the first mode as an LPB, whereas the second one represents a middle polariton branch. The exact coupling properties to the donor-bound excitons do not alter the results presented here in any way. At higher temperatures, the donor-bound exciton ionizes and vanishes. A UPB is not observable in this microcavity, as expected, due to the large absorption coefficient of the ZnO cavity in this spectral range [24, 25].

The dispersion of TE- and TM-LPB in its energy is shown in figure 3(b) for a detuning of $\Delta = -70$ meV at $T = 10$ K. As expected, the dispersion for TE- and TM-LPB is different, since the energy of the TM band of the uncoupled cavity-photon mode increases more strongly with increasing in-plane wave vector than that of the TE band. At an in-plane wave vector of $k_{\parallel} = 0.9 \times 10^7\,\mathrm{m}^{-1}$, the splitting between TE- and TM-LPB amounts to 6 meV. This is about one order of magnitude larger than that observed for GaAs- and CdTe-based microcavities [14, 16]. For larger in-plane wave vectors, the difference between the two LPBs decreases and vanishes for $k_{\parallel} > 1.2 \times 10^7\,\mathrm{m}^{-1}$. Responsible for the occurrence and position of the maximum is the change of the LPBs characteristic from a photonic to an excitonic one. At large negative detuning and small in-plane wave vectors, the LPB has a strong photonic character, which leads

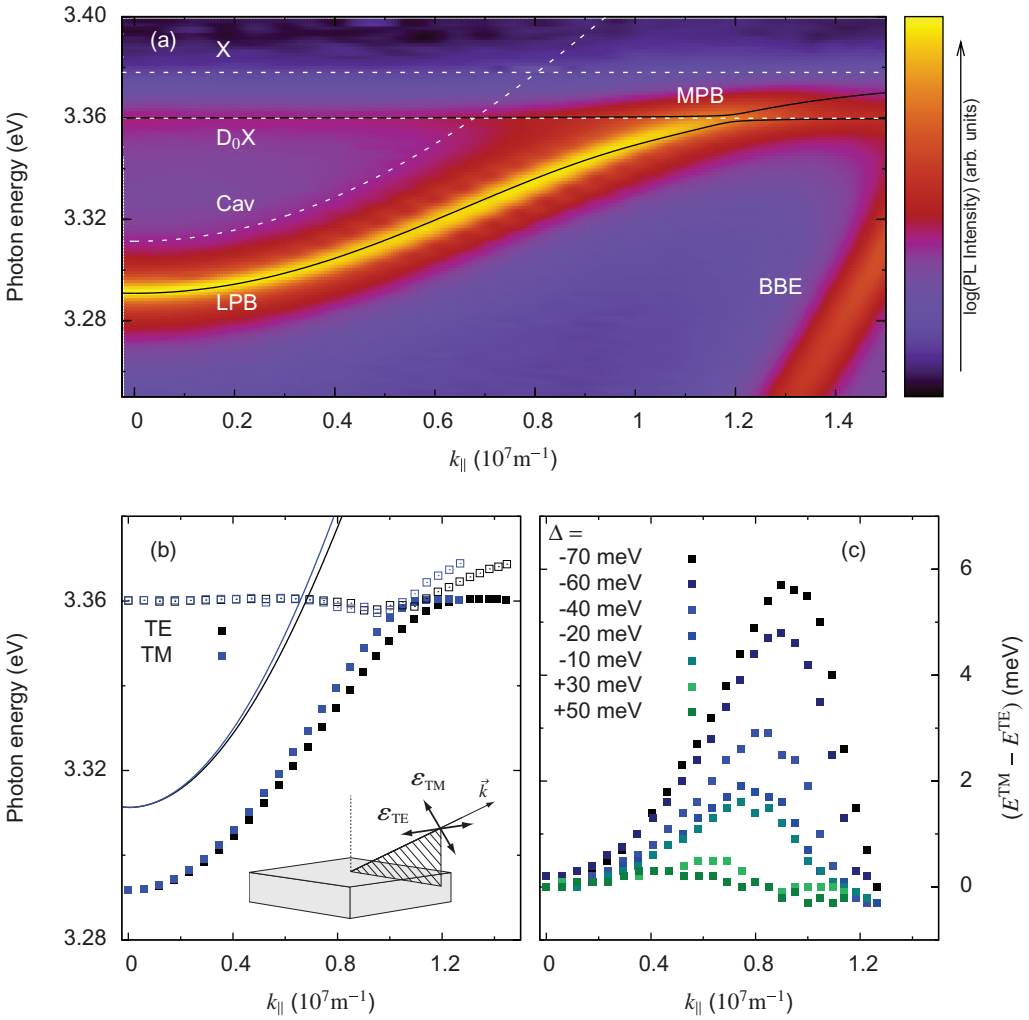

Figure 3. (a) PL spectra ($T = 10\,\mathrm{K}$) as a function of the in-plane wave vector of the emitted light in a false colour scale for a detuning of $\Delta = -70\,\mathrm{meV}$ at $T = 10\,\mathrm{K}$ for the TE-polarized light. The calculated mode energies of the LPB and MPB are shown as black solid lines, whereas the uncoupled cavity-photon mode (Cav), exciton mode (X) and the donor-bound exciton (D_0X) are shown as white dashed lines. The mode energies were calculated by using a 3×3 coupling Hamiltonian similar to that presented in [11]. For large in-plane wave vectors ($k_\parallel > 1.2 \times 10^7\,\mathrm{m}^{-1}$), the Bragg band edge mode (BBE) is observable. The dispersion of the LPB for the TE- (black symbols) and TM-polarization (blue symbols) is shown in (b). The inset shows schematically the alignment of the electric field ($\mathcal{E}$) for the TE- and TM-polarized light. The solid lines represent the dispersion of the uncoupled cavity-photon modes. The mode splitting as a function of the in-plane wave vector is shown in (c) for different detunings.

to an energy splitting between the TE- and TM-polarized cavity-photon modes, as described in section 2. At larger in-plane wave vectors, the excitonic character dominates and therefore the splitting vanishes due to the polarization independence of the excitonic mode. By increasing the detuning to positive values, the photonic character of the LPB decreases as well and the

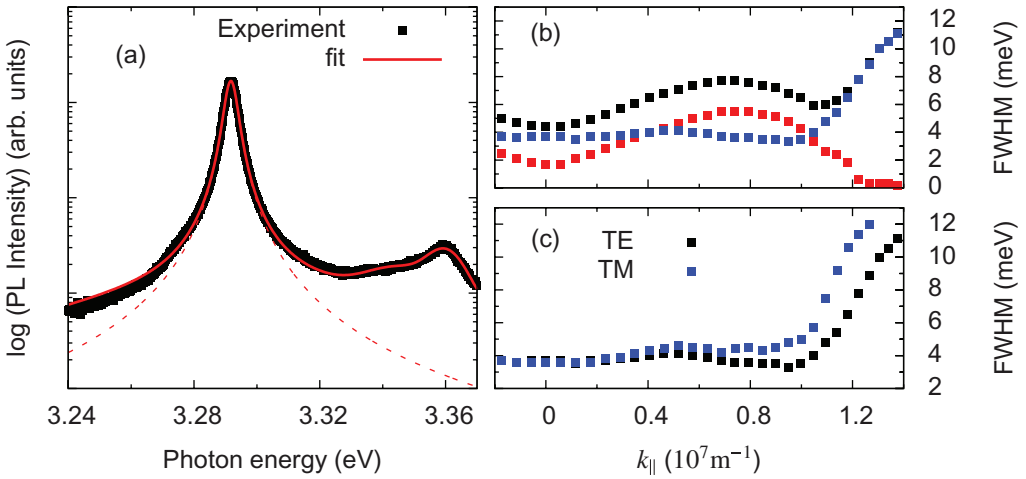

Figure 4. (a) The PL spectrum of the microresoantor at normal emission at $T = 10\,\mathrm{K}$ and $\Delta \approx -70\,\mathrm{meV}$ for the TE polarization. The black squares represent the experimental data and the red solid line the line shape analysis. The dashed red line represents the line shape of the exciton–polariton peak obtained from the line-shape analysis. (b) The dispersion behaviour of the broadening of the entire exciton–polariton peak (black squares) as well as that of the Gaussian (red squares) and the Lorentzian (blue squares) parts (same position and temperature as in (a)). (c) The dispersion behaviour of the broadening of the associated Lorentzian function for the two polarizations (the same position and temperature as in (a)).

transition from a photonic behaviour to an excitonic one shifts to smaller in-plane wave vectors. This leads to the observed decrease in the maximum of the energy splitting and its shift to smaller in-plane wave vectors (figure 3(c)). We note that the optical anisotropy of the ZnO cavity[2] affects only the TM polarization of the cavity-photon mode. From transfer matrix calculations, it can be estimated that the negative birefringence of ZnO in the discussed spectral range causes a slight enhancement of the TE–TM splitting compared with an isotropic cavity with a similar refractive index. However, due to the rotation symmetry, the cavity-photon modes for the two polarizations have degenerated in energy and lifetime at the ground state. A splitting of the ground state caused by a uniaxial in-plane strain as in CdTe-based microcavities was not observed [26].

For an ideal microcavity, the line shape of the exciton–polariton peak is Lorentzian, since, neglecting disorder or inhomogeneous scattering processes, the line shapes of the uncoupled cavity-photon mode as well as that of the exciton mode are Lorentzian. However, non-idealities, such as the scattering of the excitons with electrons, inhomogeneous strain and impurities, lead to an additional Gaussian broadening of the exciton mode. The same holds for the uncoupled cavity-photon mode, where the interface roughness between the cavity layer and the BR leads to an energy distribution of the cavity photon. Therefore, the entire broadening is a mixture of a Gaussian and a Lorentzian, and the resultant line shape can be described by a Voigt function (figure 4(a)). The broadening of the exciton–polariton peak, as well as the broadening

[2] Due to the wurtzite structure of the ZnO cavity material, the cavity is optically uniaxial with the optical axis parallel to the surface normal.

of the associated Gaussian and Lorentzian parts, is shown in figure 4 for a detuning of about $\Delta = -70\,\text{meV}$ for the TE-LPB. In general, the broadening of the entire exciton–polariton peak increases with increasing in-plane wave vector. However, for intermediate wave vectors, the broadening shows a second minimum. Responsible for this is the Gaussian part of the broadening. In contrast to the Lorentzian broadening, which is nearly constant up to an in-plane wave vector of about $1 \times 10^7\,\text{m}^{-1}$, two regimes are observable for the Gaussian part of the broadening. In the first one ($k_\parallel < 0.6 \times 10^7\,\text{m}^{-1}$), the Gaussian broadening increases with increasing in-plane wave vector, whereas for larger in-plane wave vectors (the second regime), a decrease is observable. Responsible for the two observed regimes might be that with increasing in-plane wave vector, i.e. with increasing angle of emission, the spot diameter of the detected area on the surface increases. Therefore, due to the wedge-shaped cavity, the increase in spot diameter causes an enhancement in the energy distribution of the uncoupled cavity-photon mode, which contributes to the LPB. However, for larger in-plane wave vectors (the second regime), the contribution of the cavity-photon mode to the LPB decreases, and so the broadening is mainly determined by that of the exciton. This broadening is mainly Lorentzian distributed and therefore the Gaussian broadening of the exciton–polariton peak decreases.

In the following, we discuss the Lorentzian broadening (figure 4(c)) of the TM-LPB and the TE-LPB. For small in-plane wave vectors ($k_\parallel < 0.9 \times 10^7\,\text{m}^{-1}$), a slight increase in the broadening with increasing wave vector is observable for the TM-LPB, whereas the broadening of the TE-LPB remains nearly constant. In this range, the LPB has a strong photonic character, and we relate the broadening behaviour to that of the uncoupled cavity-photon mode. For larger in-plane wave vectors, the broadening strongly increases for both polarizations since the LPB becomes excitonic and the broadening is determined by the donor-bound excitons. The in-plane wave vector at which the broadening strongly increases is slightly different for the two polarizations. For the TM-LPB, this wave vector is smaller than for the TE-LPB. This is caused by the different energy dispersion of the related uncoupled cavity-photon modes, which causes different in-plane wave vectors for the resonance with the donor-bound exciton.

In the context of exciton–polariton spin dynamics, such microcavities with a very high TE–TM splitting are of special interest. A high splitting causes a large effective magnetic field acting on the pseudospin states and therefore a pronounced energy separation of the pseudospin up and down states [27, 28]. The quantity to which the field strength is related is the dimensionless quantity $\beta_{\text{LT}} = (E^{\text{TE}} - E^{\text{TM}})/\Gamma$, with Γ being the decay rate. However, due to the cw excitation in our experiments, only the radiative part of the decay rate is accessible (Γ_{rad}) and β_{LT} cannot be determined easily from these experiments. For large negative detunings, the LPB is mainly photonic and the non-radiative decay is negligible, i.e. $\Gamma \approx \Gamma_{\text{rad}}$. The corresponding β_{LT} is shown in figure 5 for a detuning of $\Delta = -70\,\text{meV}$ for the two polarizations. Since the lifetimes of the cavity photons differ for the two polarizations, the magnitude of β_{LT} depends on the polarization. It is larger for the TE polarization than for the TM polarization. However, for both polarizations, the magnitude of β_{LT} is similar to that of GaAs-based microcavities [28] so that spin polarization effects, such as the optical spin Hall effect, should be observable in ZnO-based microcavities.

4.2. Occupation of the exciton–polariton branch

Besides energy and broadening of the exciton–polariton mode, the PL spectra allow us to deduce information about the occupation of the LPB and therewith information about relaxation

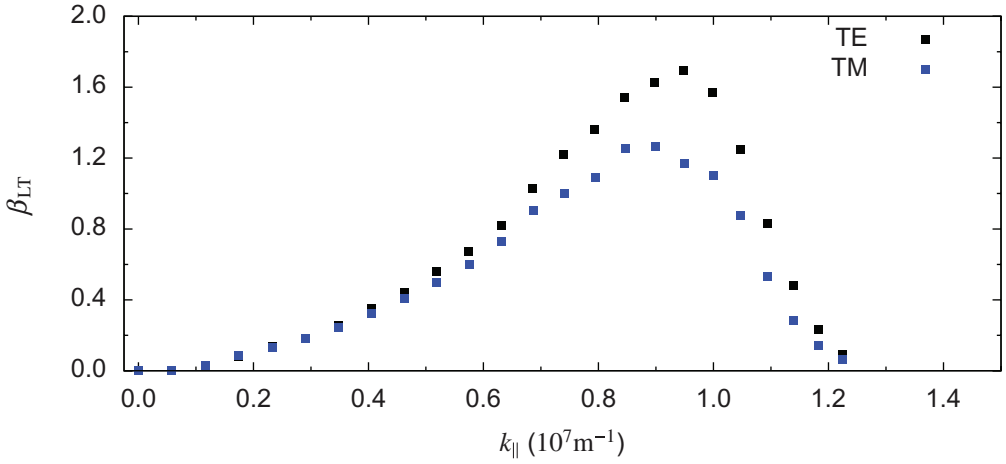

Figure 5. The relative strength of the TE–TM splitting ($\beta_{LT} = (E^{TE} - E^{TM})/\Gamma$) for the ZnO-based microcavity at $T = 10\,K$ for a detuning of $\Delta = -70\,meV$. Thereby we used for the TE polarization Γ_{TE} and for the TM polarization Γ_{TM}.

processes. In the steady-state regime, the occupation number (N) of the exciton–polaritons at an in-plane wave vector $k_\parallel$ is obtained from the Boltzmann equation for bosonic particles [29] by

$$0 = -\Gamma N_{k_\parallel} - W_{out} N_{k_\parallel} + W_{in}(1 + N_{k_\parallel}) + P_{k_\parallel}. \tag{2}$$

Thereby, Γ represents the decay rate of the exciton–polaritons, W_i the scattering rate into (in) and out of (out) a state with an in-plane wave vector $k_\parallel$ and $P_{k_\parallel}$ the generation of exciton–polaritons by the pumping. For the range of in-plane wave vectors investigated here, the generation term $P_{k_\parallel}$ can be neglected, since the excitation was done at an energy of $E_{exc} = 3.815\,eV$, which is well above the energies of the LPB. For small in-plane wave vectors and low excitation densities, the difference in the scattering rates is much smaller than the decay rate[3] ($W_{out} - W_{in} \ll \Gamma$), and therefore the ratio of the occupation numbers between two in-plane wave vectors can be approximated by

$$\frac{N_{k_{\parallel,1}}}{N_{k_{\parallel,2}}} = \frac{\Gamma_{k_{\parallel,2}}}{\Gamma_{k_{\parallel,1}}} \frac{W_{in,k_{\parallel,1}}}{W_{in,k_{\parallel,2}}}. \tag{3}$$

The index $i = 1, 2$ denotes the different in-plane wave vectors. Hereby we neglect an interaction between the TE-LPB and the TM-LPB, i.e. exciton–polaritons of TE-LPB do not scatter into the TM-LPB and vice versa.

To deduce the scattering rate into a state with an in-plane wave vector $k_\parallel$ from the PL measurements, equation (3) has to be modified. Thereby, we use the fact that at small in-plane wave vectors, the decay rate of the exciton–polaritons is mainly determined by the radiative decay (Γ_{rad}), i.e. the non-radiative decay rate is negligible, and the integrated PL peak intensity (I_{PL}) is proportional to $N\Gamma_{rad}$. This leads to a relative input scattering rate ($W_{in}^{rel}(k_\parallel)$) into a state with an in-plane wave vector $k_\parallel$, which we relate to the rate at zero in-plane wave vector,

$$W_{in}^{rel}(k_\parallel) = \frac{I_{PL}(k_\parallel)}{I_{PL}(k_\parallel = 0)} = \frac{W_{in,k_\parallel}}{W_{in,k_{\parallel}=0}}. \tag{4}$$

[3] This assumption can be roughly verified by calculating the scattering rates W_{in} and W_{out} by the approach suggested by Porras *et al* [30].

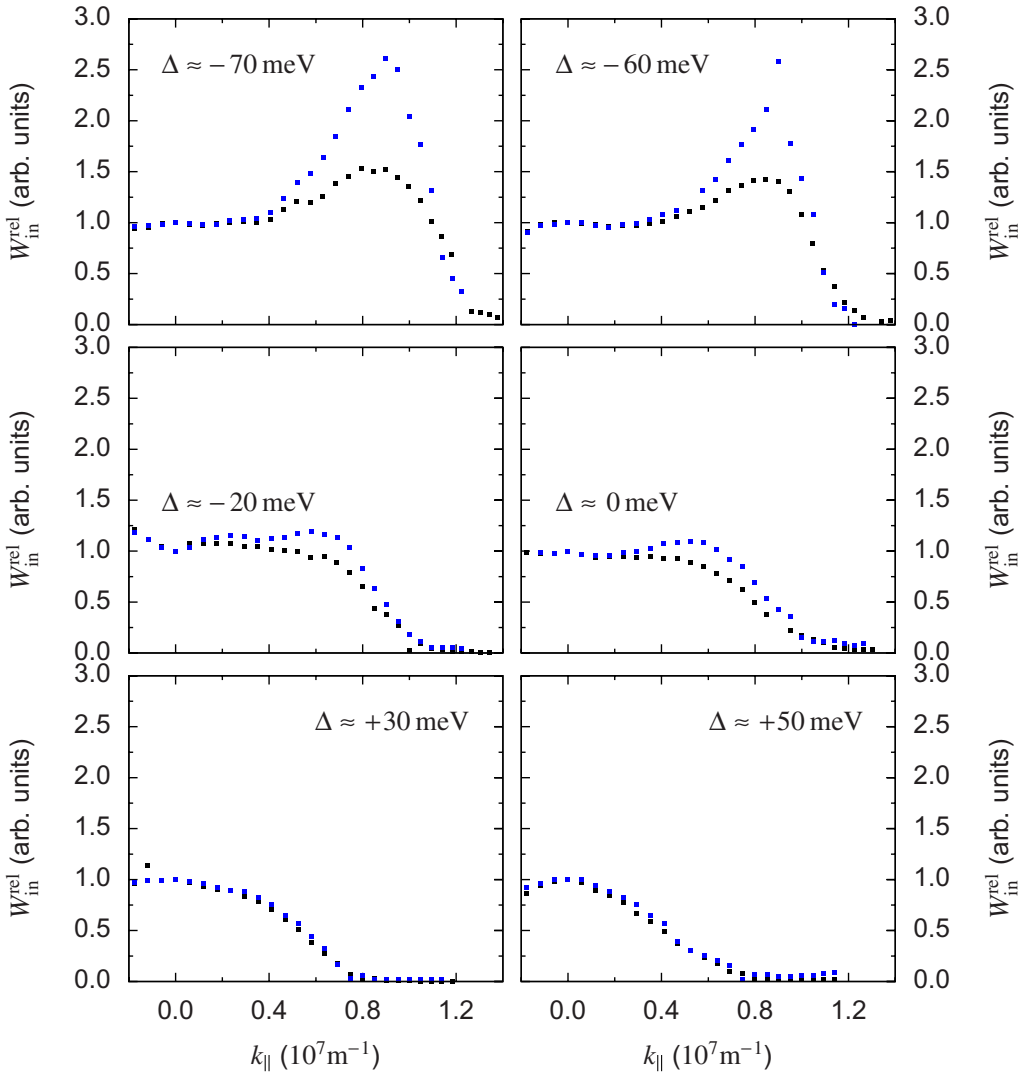

Figure 6. The relative input scattering rate W_{in}^{rel} for different detunings Δ for the TE-LPB (black squares) and the TM-LPB (blue squares). The excitation density was about 200 mW cm^{-2} and the spot size on the sample was about 200 μm (the laser beam was unpolarized).

For selected detunings, the relative input scattering rate (W_{in}^{rel}) is shown in figure 6 for TE- and TM-LPB. Thereby, only the Lorentzian part of the experimentally observed PL peak was used, which was obtained by deconvolution of the entire LP peak by using Lorentzian and Gaussian broadening, and we normalize the area of the Gaussian peak to one. For negative detunings, the maximum of W_{in}^{rel} is observable for non-zero in-plane wave vectors ($k_{\|} \approx 0.8 \times 10^7$ m^{-1} for $\Delta \approx -70$ meV) close to the bottleneck region. This indicates that scattering of exciton–polaritons into the states with these in-plane wave vectors is dominant over scattering into the ground state. This we attribute to the fact that the exciton–polaritons can relax very fast into the bottleneck region [30]–[33]. For smaller in-plane wave vectors, the relaxation time is enhanced and is much larger than their lifetime. Therefore W_{in}^{rel} decreases with decreasing in-plane wave vectors.

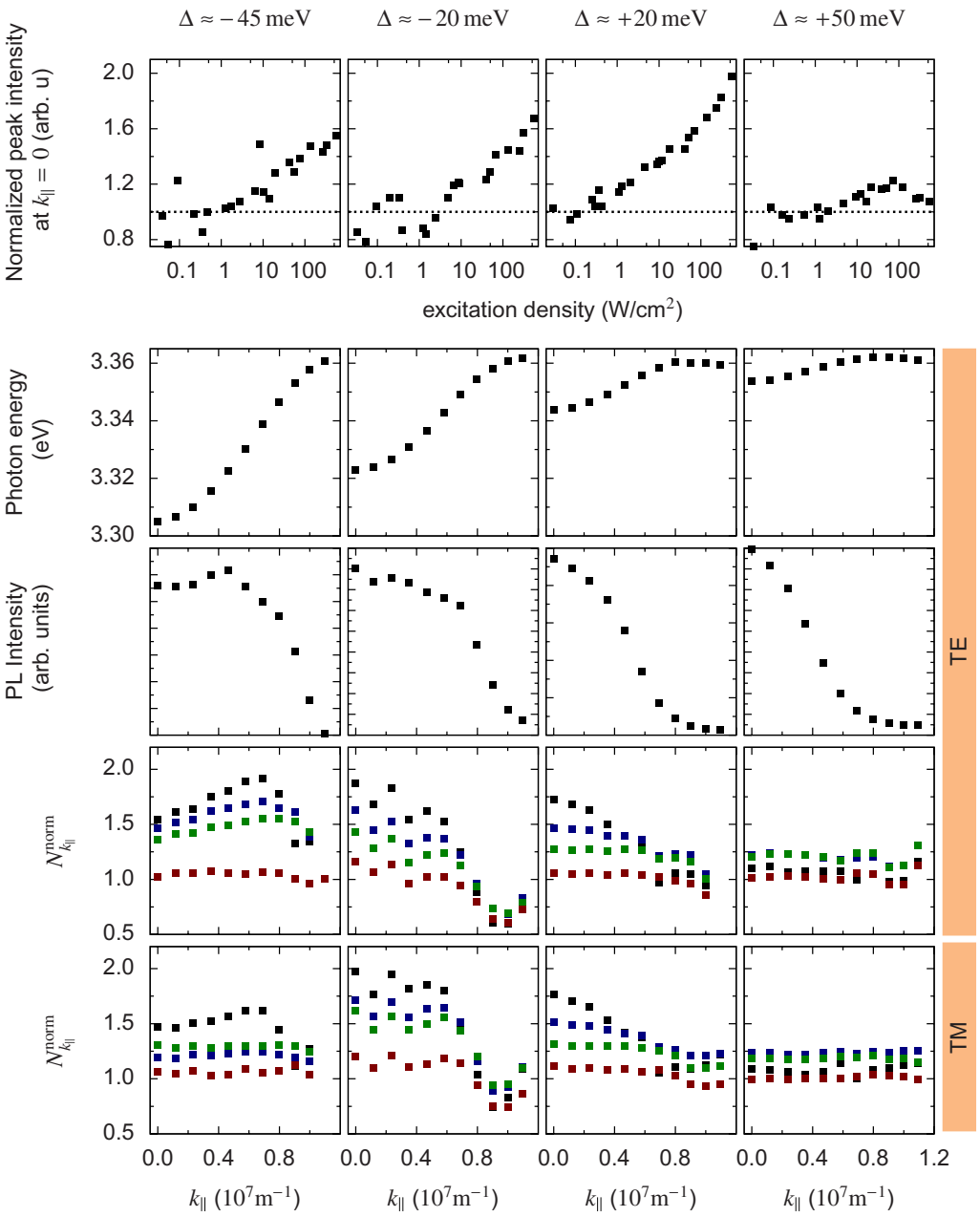

Figure 7. Top part: normalized peak intensity in dependence on the excitation density (normalized with respect to the emission at low excitation densities) of the lower polariton emission with an in-plane wave vector of $k_{\parallel} = 0$. The dashed line is a guide to the eye and represents a linear dependence of the peak intensity on the excitation density. Bottom part: the dispersion of the lower polariton branch and the change in the occupation number (normalized to the excitation density of $P = 45\,\mathrm{mW\,cm^{-2}}$) as a function of the excitation density (black squares: $P = 500\,\mathrm{W\,cm^{-2}}$; blue squares: $P = 130\,\mathrm{W\,cm^{-2}}$; green squares: $P = 40\,\mathrm{W\,cm^{-2}}$; red squares: $P = 2\,\mathrm{W\,cm^{-2}}$). (The laser beam was linearly polarized, i.e. the electric field vector was parallel to the layer interface of the microcavity.)

A comparison of the relative input scattering rates between the TE- and TM-LPB yields that $W_{\mathrm{in}}^{\mathrm{rel}}$ is, at the bottleneck region, larger for the TM-LPB than for the TE-LPB. This finding we relate to the difference in the dispersion behaviour of the two LPBs. Due to the fact that both LPBs coincide at zero in-plane wave vector and converge to the same energy at large in-plane wave vectors, the curvature at the bottleneck region is smaller for the TE-LPB than for the TM-LPB (cf figure 3(b)). The smaller curvature of the TE-LPB supports the relaxation process of the exciton–polaritons into the lower states, since the energy and momentum conservation can be more easily fulfilled than for a large curvature. Therefore, compared with the lower states, the input scattering rate is, at the bottleneck region, larger for the TM-LPB than for the TE-LPB, as we have observed.

By increasing the detuning to positive values, the excitonic character of the LPB increases, whereas the photonic one decreases. This leads, on the one hand, to a reduction in the bottleneck and, on the other hand, to a reduction in the polarization splitting. Therefore, the maximum of the relative input scattering rate $W_{\mathrm{in}}^{\mathrm{rel}}$ shifts to smaller in-plane wave vectors with increasing detuning and the difference in the scattering rate between the TE-LPB and TM-LPB decreases. These findings would indicate that a positive detuning is preferred in order to reach an accumulation of exciton–polaritons at the ground state, as suggested by Johne *et al* [33].

To verify that positive detunings are preferred in order to reach an accumulation of exciton–polaritons at the ground state, we carried out measurements with different excitation densities. Assuming that the decay rate (and also the Gaussian broadening) at a given in-plane wave vector is independent of the excitation density P, the change in the exciton–polariton occupation number between two different excitation densities can be deduced from the integrated PL peak intensity by

$$N_{k_\parallel}^{\mathrm{norm}} = \frac{N_{k_\parallel}(P = P_1)}{N_{k_\parallel}(P = P_2)} = \frac{I_{\mathrm{PL}}(P = P_1)}{I_{\mathrm{PL}}(P = P_2)}. \tag{5}$$

This ratio represents a normalized occupation number. In the linear regime, where the occupation number depends linearly on the excitation density, the normalized occupation number should be 1.

For selected temperatures and detunings, the normalized emission intensity of the ground state and the normalized occupation number of the LPB for different excitation densities is shown in figure 7. At low temperatures ($T = 10\,\mathrm{K}$), we observe a superlinear enhancement of the ground-state emission intensity with increasing excitation density for detunings smaller than $\Delta = +50\,\mathrm{meV}$. A comparison of the occupation of the LPB for all recorded in-plane wave vectors yields that the strongest enhancement of the occupation with increasing excitation density is obtained in the bottleneck region instead of in the ground state for a detuning of $\Delta \approx -45\,\mathrm{meV}$. This enhancement is stronger for the TE-LPB than for the TM-LPB. In this detuning regime, the pronounced change in the LPB dispersion with $k_\parallel$ is prejudicial for the relaxation of hot carriers into the ground state. Therefore, the relaxation of hot carriers in the bottleneck region is the fastest process in this regime. This leads to the observed accumulation of exciton–polaritons in the bottleneck region for this detuning regime. Responsible for the different enhancement of the occupation for the TE- and TM-LPB might be the fact that the TM-LPB already shows a larger occupation for low excitation densities than the TE-LPB. With increasing excitation density, the occupation of the LPB for both polarizations increases. At the same time, the scattering of exciton–polaritons into the ground state increases, since the exciton–polariton scattering rate, which is highly efficient, increases with increasing

exciton–polariton density. This scattering rate is larger for the TM-LPB than for the TE-LPB due to the larger occupation number of the TM-LPB at the bottleneck region and leads to the observed pronounced accumulation of the exciton–polaritons in the TE-LPB. For small in-plane wave vectors, the TE-LPB and the TM-LPB coincide with each other and therefore the same occupation is observed for the two polarizations.

For an intermediate detuning regime ($-20\,\mathrm{meV} < \Delta < +20\,\mathrm{meV}$), the bottleneck effect is reduced, since the change in the dispersion behaviour is smaller than that at negative detuning. The superlinear behaviour of the exciton–polariton occupation number with increasing excitation density is also observable for the states at the bottleneck region and below. The strongest enhancement is observable for the ground state, which yields an enhancement of the normalized occupation by a factor of 2. In this detuning regime, the change in the curvature of the LPB is reduced compared with the negative one and therefore the hot exciton–polaritons can relax very fast into the ground state. Unfortunately, a macroscopic occupation with exciton–polaritons was not achieved. Responsible for this might be the large spot diameter on the surface of the microcavity of about $100\,\mu$m and/or a missing potential acting as a trap to capture the exciton–polaritons.

For large positive detuning ($\Delta \approx +50\,\mathrm{meV}$), a superlinear enhancement of the occupation at the ground state or at the bottleneck region is not observable. In this detuning regime, the dispersion of the LPB is very flat, which would be beneficial for the relaxation into the ground state. However, this would also reduce the optical trap formed by the change in the LPB dispersion, which would capture the exciton–polaritons and prevent an escape of the exciton–polaritons out of the ground state. Therefore, the exciton–polaritons can leave the ground state easily due to their thermal energy. This process would counteract the formation of a high occupation of the ground state and lead to an enhancement of the critical density for the formation of a BEC. A similar behaviour was also found in GaN-based microcavities by Butté *et al* [12].

A difference in occupation between the TE-LPB and TM-LPB was not observable for the last two detuning regimes, since the energy splitting between the TE-LPB and TM-LPB and the difference in their occupation are for these two detuning regimes very small. The energy of the LPB as well as its broadening remain nearly the same for all detuning regimes for excitation densities less than $130\,\mathrm{W\,cm^{-2}}$. For larger exciton-densities, we observe a small redshift of the LPB energy of about 1 meV and an increase in broadening of about 0.5 meV at $P \approx 500\,\mathrm{W\,cm^{-2}}$ for a detuning of $\Delta \approx +50\,\mathrm{meV}$. This we attribute to a warming of the microcavity. The strong coupling regime is also observable for these excitation densities. For smaller detuning, the redshift and the increase in broadening are smaller. For these detunings, the properties of the uncoupled cavity-photon mode contribute more strongly to the LPB than for large positive detuning, which are not so strongly affected by the temperature [11].

To summarize, these findings indicate that at low temperatures ($T = 10\,\mathrm{K}$), an intermediate detuning regime ($-20\,\mathrm{meV} < \Delta < +20\,\mathrm{meV}$) is preferred in order to reach an accumulation of exciton–polaritons at the ground state.

By increasing the temperature, the scattering rates of the exciton–polaritons into and out of a state with a certain in-plane wave vector increase and therefore the approximation $W_{\mathrm{out}} - W_{\mathrm{in}} \ll \Gamma$ cannot be applied. Therefore, only the occupation number is a meaningful quantity. Figure 8 shows the occupation number ($N_{k_\parallel} \propto I_{\mathrm{PL},k_\parallel} / \Gamma_{\mathrm{rad},k_\parallel}$) of the TM-LPB for temperatures up to $T = 130\,\mathrm{K}$ for a detuning of $\Delta \approx -60\,\mathrm{meV}$. Thereby we use only the Lorentzian fraction of the exciton–polariton peak, as described above, and assume that Γ_{rad} is proportional to the

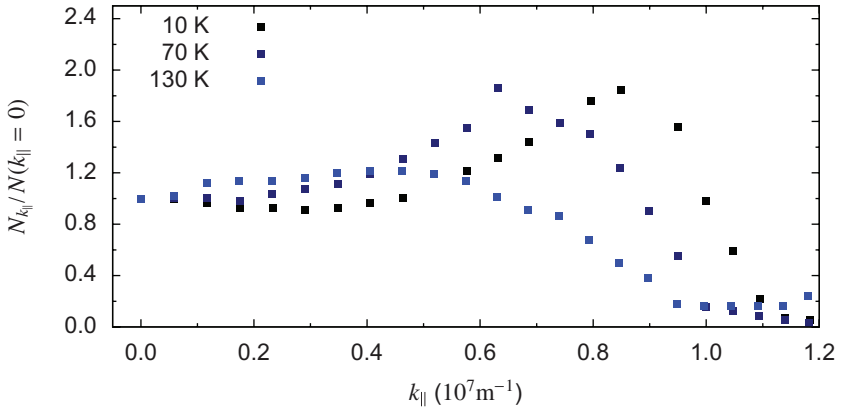

Figure 8. The occupation number for the TM-LPB for a *detuning of* $\Delta \approx -60$ meV. (The laser beam was unpolarized.)

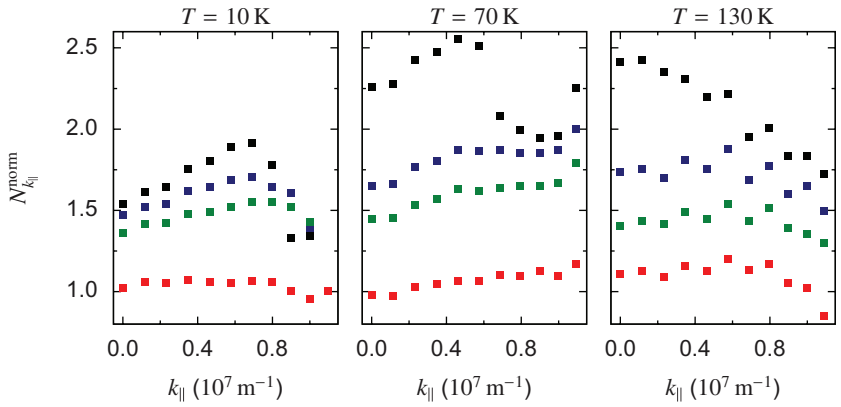

Figure 9. The occupation number (normalized with respect to the excitation density) (equation (5)) of the lower polariton branch (TE-polarized) at a detuning of $\Delta \approx -45$ meV for different temperatures (black squares: $P = 500\,\mathrm{W\,cm^{-2}}$; blue squares: $P = 130\,\mathrm{W\,cm^{-2}}$; green squares: $P = 40\,\mathrm{W\,cm^{-2}}$; red squares: $P = 2\,\mathrm{W\,cm^{-2}}$). (The laser beam was linearly polarized, i.e. the electric field vector was parallel to the layer interface of the microcavity.)

Lorentzian broadening. We show only data for temperatures up to 130 K, because at higher temperatures, not all detuning regimes can be realized with our microcavity. With increasing temperature, a reduction in the bottleneck occupation is observable and the difference between the occupation in TM-LPB and TE-LPB decreases. These findings indicate an enhancement of the exciton–polariton scattering rate into the ground state at higher temperatures, which is in agreement with numerical calculations [30, 31].

The enhancement of the input scattering rate with increasing temperature causes the detuning regime, which is preferred for an accumulation of exciton–polaritons at the ground state, to shift to larger negative detuning values. By increasing the temperature, we observe an enhancement of the superlinear growth of the exciton–polariton occupation at small in-plane wave vectors for the negative detuning regime (figure 9). For a temperature of $T = 130$ K, the strongest enhancement of the exciton–polariton occupation is obtained at a zero in-plane wave vector. Here, the normalized occupation increases by a factor of about 2.5.

5. Summary

We have investigated the occupation of the lower polariton branch in a ZnO-based microcavity as a function of the polarization of the emitted light as well as on the detuning and temperature. We have observed an energy splitting between the TE- and TM-polarized lower polariton branches of about 6 meV ($\Delta \approx -70$ meV), which is caused by the dispersion of the related uncoupled cavity-photon modes. This energy splitting is about one order of magnitude larger than that of the conventionally used microcavities based on CdTe and GaAs and it causes a difference in the input scattering rates into the lower polariton branch for the two polarizations. The scattering into the bottleneck region of the lower polariton branch is much stronger for the TM-polarized light than for the TE-polarized light at negative detunings. This difference in the input scattering rates increases with increasing negative detuning. From the excitation density-dependent measurements, we conclude that large negative detunings are preferred in order to reach an enhancement of the exciton–polariton occupation at the ground state ($\Delta \approx -45$ meV at $T = 130$ K). For such negative detunings, the polarization dependence of the cavity-photon mode has a strong influence on the exciton–polariton scattering rates in ZnO-based microcavities and has to be considered in addition to the longitudinal-transversal splitting of the exciton to understand the scattering and relaxation mechanism in these microcavities.

Acknowledgments

We thank H Hochmuth and M Lorenz for their support during the growth of the samples. This work was supported by Deutsche Forschungsgemeinschaft within the Leipzig School of Natural Sciences BuildMoNa (GS 185/1) and the project GR 1011/20-1, and by the European Social Fund (ESF).

References

[1] Weisbuch C, Nishioka M, Ishikawa A and Arakawa Y 1992 *Phys. Rev. Lett.* **69** 3314
[2] Kavokin A, Baumberg J J, Malpuech G and Laussy F P 2008 *Microcavities* (*Semiconductor Science and Technology*) (Oxford: Oxford University Press)
[3] Saba M *et al* 2001 *Nature* **414** 731
[4] Saba M, Kundermann S, Ciuti C, Guillet T, Staehli J-L and Deveaud B 2003 *Phys. Status Solidi* b **238** 432
[5] Tsintzos S I, Pelekanos N T, Konstantinidis G, Hatzopoulos Z and Savvidis P G 2008 *Nature* **453** 372
[6] Deng H, Weihs G, Snoke D, Bloch J and Yamamoto Y 2003 *Proc. Natl Acad. Sci. USA* **100** 15318
[7] Kasprzak J *et al* 2006 *Nature* **443** 409
[8] Christopoulos S *et al* 2007 *Phys. Rev. Lett.* **98** 126405
[9] Le Si Dang, Heger D, André R, Bœuf F and Romestain R 1998 *Phys. Rev. Lett.* **81** 3920
[10] Chichibu S F *et al* 2005 *Semicond. Sci. Technol.* **20** S67
[11] Sturm C, Hilmer H, Schmidt-Grund R and Grundmann M 2009 *New J. Phys.* **11** 073044
[12] Butté R, Levrat J, Christmann G, Feltin E, Carlin J-F and Grandjean N 2009 *Phys. Rev.* B **80** 233301
[13] Özgür U, Alivov Y-I, Liu C, Teke A, Reshchikov M A, Dogan S, Avrutin V, Cho S-J and Morkoc H 2005 *J. Appl. Phys.* **98** 041301
[14] Panzarini G, Andreani L C, Armitage A, Baxter D, Skolnick M S, Astratov V N, Roberts J S, Kavokin A V, Vladimirova M R and Kaliteevski M A 1999 *Phys. Rev.* B **59** 5082
[15] Dukin A A, Feoktistov N A, Golubev V G, Medvedev A V, Pevtsov A B and Sel'kin A V 2003 *Phys. Rev.* E **67** 046602

[16] Baxter D, Skolnick M S, Armitage A, Astratov V N, Whittaker D M, Fisher T A, Roberts J S, Mowbray D J and Kaliteevski M A 1997 *Phys. Rev.* B **56** R10032
[17] Shelykh I A, Kavokin A V and Malpuech G 2005 *Phys. Status Solidi* b **242** 2271
[18] Hilmer H, Sturm C, Schmidt-Grund R, Rheinländer B and Grundmann M 2010 *Superlattices Microstruct.* **47** 19
[19] Ellmer K, Klein A and Rech B (ed) 2008 *Transparent Conductive Zinc Oxide: Basics and Applications in Thin Film Solar Cells* (*Springer Series in Materials Science*) (Berlin: Springer)
[20] Meyer B K *et al* 2004 *Phys. Status Solidi* b **241** 231
[21] Kavokin A and Malpuech G 2003 *Cavity Polaritons (Thin Films and Nanostructures* vol 32*)* (Amsterdam: Academic)
[22] Reithmaier J P, Sek G, Loffler A, Hofmann C, Kuhn S, Reitzenstein S, Keldysh L V, Kulakovskii V D, Reinecke T L and Forchel A 2004 *Nature* **432** 197
[23] Yoshie T, Scherer A, Hendrickson J, Khitrova G, Gibbs H M, Rupper G, Ell C, Shchekin O B and Deppe D G 2004 *Nature* **432** 200
[24] Faure S, Guillet T, Lefebvre P, Bretagnon T and Gil B 2008 *Phys. Rev.* B **78** 235323
[25] Médard F *et al* 2009 *Phys. Rev.* B **79** 125302
[26] Kłopotowski Ł, Martín M D, Amo A, Viña L, Shelykh I A, Glazov M M, Malpuech G, Kavokin A V and André R 2006 *Solid State Commun.* **139** 511
[27] Shelykh I A, Kavokin A V, Rubo Y G, Liew T C H and Malpuech G 2010 *Semicond. Sci. Technol.* **25** 013001
[28] Kavokin A, Malpuech G and Glazov M 2005 *Phys. Rev. Lett.* **95** 136601
[29] Uhlenbeck G E and Gropper L 1932 *Phys. Rev.* **41** 79
[30] Porras D, Ciuti C, Baumberg J J and Tejedor C 2002 *Phys. Rev.* B **66** 085304
[31] Tassone F and Yamamoto Y 1999 *Phys. Rev.* B **59** 10830
[32] Cao H T, Doan T D, Tran Thoai D B and Haug H 2004 *Phys. Rev.* B **69** 245325
[33] Johne R, Solnyshkov D D and Malpuech G 2008 *Appl. Phys. Lett.* **93** 211105